Supplementary Information (SI) for Journal of Materials Chemistry C.

Supporting information

C1-Substituted Bipolar Spiro Host for High-Performance Organic Light-Emitting Diodes

Yue-Jian Yang[ab], Qi Zheng[ab], Peng Zuo[ab], Hai-Tian Yuan[ab], Rui-Hong Liu[ab], Zi-Qi Feng[ab], Dong-Ying Zhou*[ab], Zuo-Quan Jiang*[ab] and Liang-Sheng Liao[abc]

a. Institute of Functional Nano & Soft Materials (FUNSOM), Soochow University, Suzhou, 215123 Jiangsu, P.R. China.

b. Jiangsu Key Laboratory for Carbon-Based Functional Materials & Devices, Soochow University, Suzhou, 215123, Jiangsu, P.R. China.

c. Macao Institute of Materials Science and Engineering, Macau University of Science and Technology, Taipa, 999078, Macau SAR, China.

E-mail: zqjiang@suda.edu.cn; dyzhou@suda.edu.cn

Experimental section

General information

All chemicals and reagents were used as received from commercial resources without further purification. ^{1}H NMR and ^{13}C NMR spectra were measured on a Bruker 400 at room temperature. Mass spectra were performed on a Thermo ISQ mass spectrometer using a direct exposure probe. Matrix-assisted laser desorption/ionization time-of-flight mass spectrometry (MALDI-TOF-MS) was performed on Bruker Autoflex II/Compass 1.0.

Differential scanning calorimetry (DSC) was performed on a TA DSC 2010 unit at a heating rate of 10 °C/min under nitrogen. The glass transition temperature (T_g) was determined from the second heating scan. Thermogravimetric analysis (TGA) was performed on the TA SDT 2960 instrument at a heating rate of 10 °C/min under nitrogen, the temperature at 5% weight loss was used as the decomposition temperature (T_d).

The electrochemical measurement was made using a CHI600 voltammetric analyzer. A conventional three-electrode configuration consisting of a platinum working electrode, a Pt-wire counter electrode, and an Ag/AgCl reference electrode was used. The solvent in the measurement was CH_2Cl_2, and the supporting electrolyte was 0.1 M tetrabutylammonium hexafluorophosphate. Ferrocene was added as a calibrant after each set of measurements, and all potentials reported were quoted regarding the ferrocene ferrocenium (Fc/Fc^+) couple at a scan rate of 100 mV/s.

The ultraviolet-visible (UV–vis) absorption spectra were recorded on a Shimadzu UV 2600 spectrophotometer. Photoluminescence (PL) spectra and phosphorescent spectra were performed on Hitachi F-4600 fluorescence spectrophotometer and HORIBA FL-1000 fluorescence spectrophotometer.

All density functional theory (DFT) calculation was carried out using Gaussian 16 C.01 software package[1] and ORCA 5.0 software package.[2] The gas-phase ground state geometry optimizations were performed at ωb97xd/def2-SVP level with the ω value of 0.12.[3, 4] Then time-dependent DFT (TD-DFT) calculation was adopted at ω-tuned TDA-ωb97xd/def2-SVP level to optimize geometries of excited states.

Crystals were picked up with a cryoloop and then frozen at 150 K or 170 K under a stream of dry N_2. Data were collected on a D8 VENTURE Bruker AXS diffractometer with CuKα radiation (λ = 1.54178 Å).

Structures were solved by direct methods (SIR92) and refined (SHELXL-2014/7) by full-matrix least-squares methods as implemented in the WinGX software package. An empirical absorption (multi-scan) correction was applied. Hydrogen atoms were introduced at calculated positions (riding model) included in structure factor calculation but not refined. Refinement parameters are summarized in Table S1.

Crystallographic data have been deposited with the Cambridge Crystallographic Data Centre as supplementary publication data: **STFPPO** (CCDC 2402740). Copies of the data can be obtained free of charge by application to CCDC, 12 Union Road, Cambridge CB2 1EZ, UK [fax: (+44) 1223-336-033; e-mail: deposit@ccdc.cam.ac.uk].

Figures were generated with Mercury software 2023, 2.0.

Device fabrication and measurement

The OLEDs were fabricated by vacuum deposition technology. All the functional layers were fabricated on pretreated ITO substrates. The glass substrates coated with ITO layers were sequentially cleaned ultrasonically with acetone and ethanol and then dried in an oven at 110 °C for 1 h. After being treated with ultraviolet–ozone plasma, the substrates were transferred into the evaporating chamber. OLED devices were fabricated through vacuum deposition under 4×10^{-6} Torr. After the deposition of functional layers, OLED device characterization was carried out at room temperature. EL spectra, luminance, and current density–voltage–luminance characteristics were measured under a constant source Keithley 2400 Source Meter and Photo Research PR 745 spectrophotometer.

Thermal properties

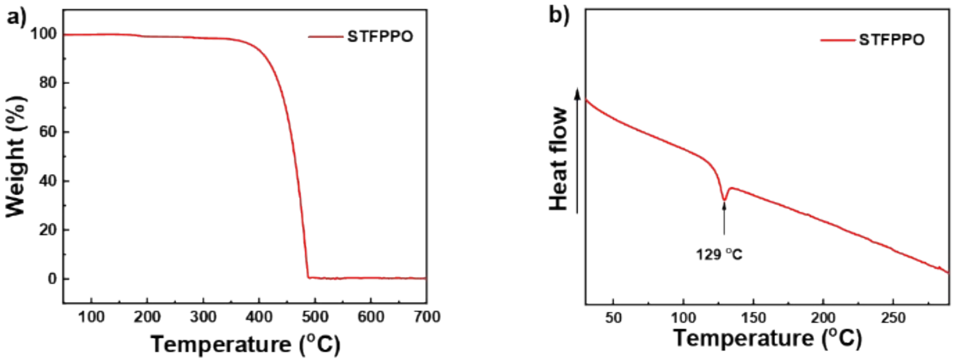

Figure S1. a) TGA and b) DSC curves of **STFPPO.**

Electrochemical properties

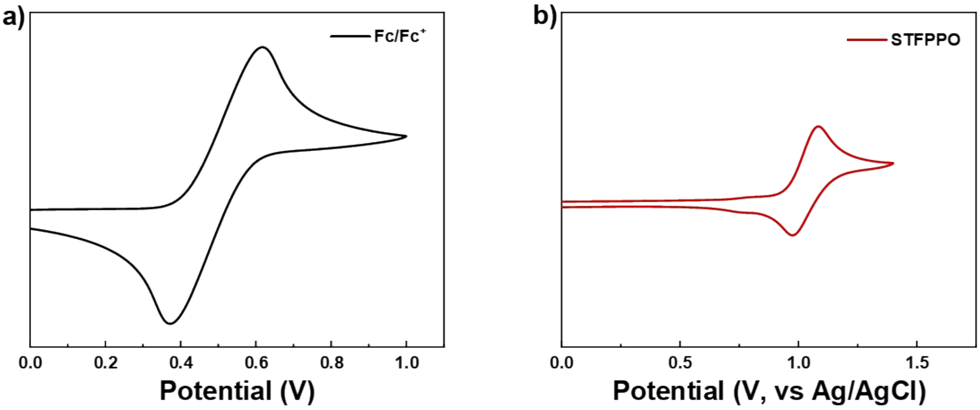

Figure S2. a) CV curve of ferrocene; and b) Cyclic voltammetry of **STFPPO** in CH_2Cl_2 for oxidation.

Table S1. Crystal parameters for **STFPPO**.

Identification code	**STFPPO**
Empirical formula	$C_{50}H_{36}Cl_2NOP$
Formula weight	768.67
Temperature/K	100
Crystal system	monoclinic
Space group	$P2_1/c$
a/Å	20.8484(8)
b/Å	9.0068(4)
c/Å	21.5551(9)
α/°	90
β/°	108.864(3)
γ/°	90
Volume/Å^3	3830.2(3)
Z	4
ρ_{calc}g/cm^3	1.333
μ/mm^{-1}	2.230
F(000)	1600.0

Crystal size/mm^3	0.09 × 0.05 × 0.04
Radiation	CuKα (λ = 1.54178)
2Θ range for data collection/°	8.374 to 127.36
Reflections collected	6094
Independent reflections	6094 [R_{int} = 0, R_{sigma} = 0.1350]
Data/restraints/parameters	6094/0/496
Goodness-of-fit on F^2	1.048
Final R indexes [I>=2σ (I)]	R_1 = 0.0888, wR_2 = 0.2330
Final R indexes [all data]	R_1 = 0.1351, wR_2 = 0.2599
Largest diff. peak/hole / e Å^{-3}	0.62/-0.74

DFT Calculation

Table S2. Cartesian coordinates of optimized STFPPO:

P	-3.71986900	-0.14685100	-0.43874500
O	-3.73105900	0.85566200	-1.53495800
N	1.26514400	1.87876200	-0.50574800
C	0.06862800	-1.35475400	-1.19765400
H	0.74050200	-1.30419600	-2.05476000
C	1.43984500	1.44521500	0.82828200
C	1.88704200	1.22702400	-1.56966700
C	2.33808700	0.39684900	1.11821300
C	-4.87580600	-2.68859200	-0.01094700
H	-4.23926200	-2.79083600	0.87030100
C	-1.18939800	-0.78725000	-1.27793100
H	-1.50086100	-0.26656300	-2.18690500
C	3.00303700	-1.83293300	0.17061600
C	0.42445300	3.03102500	-0.76476300
C	0.48094000	-1.99928500	-0.02728200
C	2.80518000	0.18311000	-1.36036500
C	1.84186200	-2.60521600	0.12700700
C	3.38524000	-0.45041000	-2.45418900
H	4.09661200	-1.26016800	-2.27324500

C	4.65352900	-0.14934700	0.30263700
C	-0.94790500	2.87880900	-0.89180700
H	-1.40257200	1.89127200	-0.81331500
C	1.01644700	4.27237300	-0.90378000
H	2.09925900	4.36817700	-0.80701100
C	0.72432500	2.04803900	1.85978700
H	0.03416300	2.86112200	1.63707700
C	4.24273400	-2.42172700	0.47304100
C	1.77992400	0.61013600	3.47284500
H	1.91995900	0.28333600	4.50477300
C	2.47904500	0.00703200	2.45415800
H	3.17702400	-0.80247500	2.68384900
C	-4.83440700	-1.53507600	-0.80130500
C	-2.07535200	-0.86736200	-0.20807400
C	-0.41346400	-2.07932500	1.04051900
H	-0.09296200	-2.56610400	1.96451400
C	-4.18724700	0.53565800	1.15700700
C	3.15018600	-0.31340300	0.04400500
C	2.14049700	0.94556700	-3.95267100
H	1.86670600	1.24330700	-4.96771600
C	5.25174300	-1.37960700	0.58237500
C	-1.67585400	-1.53420400	0.95598400
H	-2.34441900	-1.58736900	1.81933400
C	1.57326900	1.58594000	-2.89907400
H	0.84810800	2.38014200	-3.07557300
C	1.96346300	-3.98786100	0.30597300
H	1.06402000	-4.60588700	0.25565600
C	5.40106100	1.01372900	0.27976200
H	4.92829900	1.96922600	0.03976300
C	0.21464800	5.37313100	-1.17591900

H	0.67530100	6.35637900	-1.29721600
C	-1.15089600	5.23345100	-1.29145000
H	-1.77445700	6.10488900	-1.50252500
C	0.89359700	1.63148600	3.17019700
H	0.32545800	2.12261500	3.96358100
C	3.19320600	-4.57491000	0.54136000
H	3.25786700	-5.65782100	0.66868100
C	-1.73552300	3.98356100	-1.13438600
H	-2.81441400	3.84772400	-1.23423300
C	-5.49668600	0.47315600	1.64938900
H	-6.25252900	-0.10132700	1.10693100
C	-3.25993300	1.28574800	1.87919700
H	-2.22789000	1.35444700	1.52178300
C	4.34563500	-3.79837600	0.65705600
H	5.30764000	-4.26211900	0.88548600
C	-5.64347100	-1.42548600	-1.92152900
H	-5.57872700	-0.51591300	-2.52405700
C	-5.73853700	-3.72046100	-0.37392500
H	-5.77286100	-4.62820500	0.23326500
C	3.07015000	-0.08423200	-3.76166700
H	3.53041300	-0.59271400	-4.60983300
C	6.61415900	-1.42905300	0.89518200
H	7.09329700	-2.38268900	1.12979000
C	-6.54452400	-3.61035900	-1.48335300
H	-7.21458900	-4.43099900	-1.75055700
C	6.76909200	0.94798100	0.57786700
H	7.36690800	1.86181800	0.56759700
C	-6.51095500	-2.45970500	-2.27291300
H	-7.14695700	-2.37074900	-3.15552700
C	-5.84256200	1.13363500	2.80532000

H	-6.87146900	1.07569800	3.16820300
C	-4.90079200	1.85650300	3.52224300
H	-5.18028300	2.36743300	4.44575600
C	-3.59823100	1.92304500	3.04247000
H	-2.84011900	2.48900000	3.58823800
C	7.35321200	-0.25782800	0.89821500
H	8.41720400	-0.29697800	1.14262900

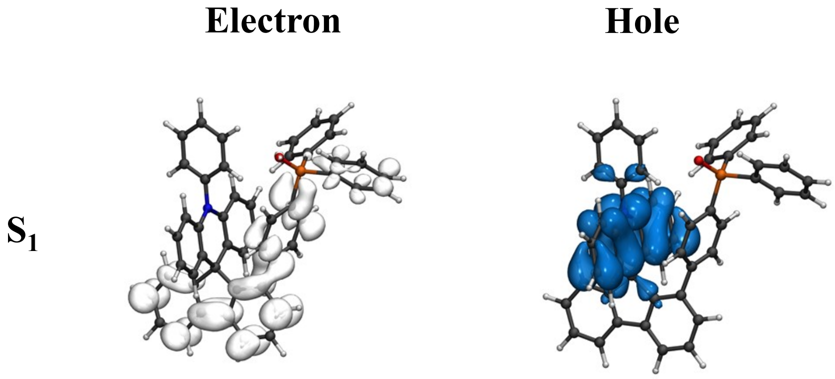

Figure S3. Hole-electron distribution of **STFPPO** for the first excited singlet state obtained by TD-DFT.

Charge mobility

Space-charged limited current (SCLC) diodes.

The device configuration of the electron-only device (EOD) is ITO/Liq (2 nm)/ STFPPO (100 nm)/ /Liq (2 nm)/Al (80 nm), and the hole-only device (HOD) is ITO/HAT-CN (10 nm)/STFPPO (100 nm)/ HAT-CN (10 nm)/Al (80 nm). After the fabrication, the devices were encapsulated before testing in dark.

The *J*–*V* curves of charge-only devices show the charge transport ability of the compound. Based on the Schottky thermionic region and space-charge-limited current (SCLC) model, the curves can be divided into two parts under low bias. We assign the second region of the *J*–*V* curve as assigned as the SCLC region, which then can be described by an equation:

$$J = \frac{9}{8}\varepsilon\varepsilon_0\mu_0 exp(\beta\sqrt{\frac{V}{L}})\frac{V^2}{L^3}$$

in which V is the driving voltage, L is the thickness of the thin layer, ε_0 is the permittivity of the free space, ε is the relative dielectric constant (estimated to be 3.0 here), μ_0 is the zero-field mobility and β is Poole-Frenkel factor. The thickness L equals to 100 nm.

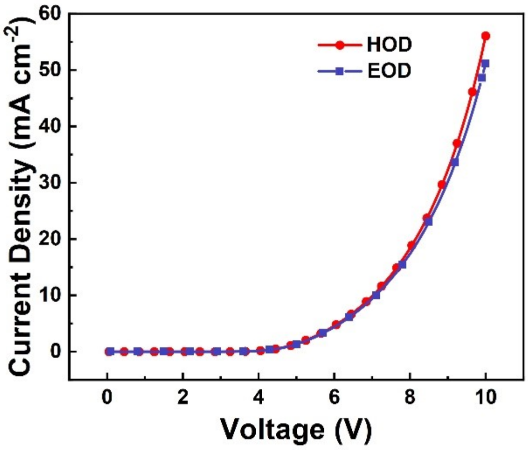

Figure S4. The *J*–*V* curve of electron-only (EOD) and hole-only (HOD) devices with host material **STFPPO**.

Electroluminescent properties

The configurations of devices are shown below: PHOLED: ITO/HAT-CN (10 nm)/TAPC (40 nm)/TCTA (10 nm)/mCP (10 nm)/Host: FIrpic (15 wt%, 20 nm)/TmPyPB (40 nm)/Liq (2 nm)/Al (80 nm) and MR-TADF OLED: ITO/ HAT-CN (10 nm)/ TAPC (40 nm)/ TCTA (10 nm)/ mCP (10 nm)/ Host: 15 wt% FIrpic： 2 wt% BNCz (20 nm)/ TmPyPB (40 nm)/ Liq (2 nm)/ Al (80 nm).

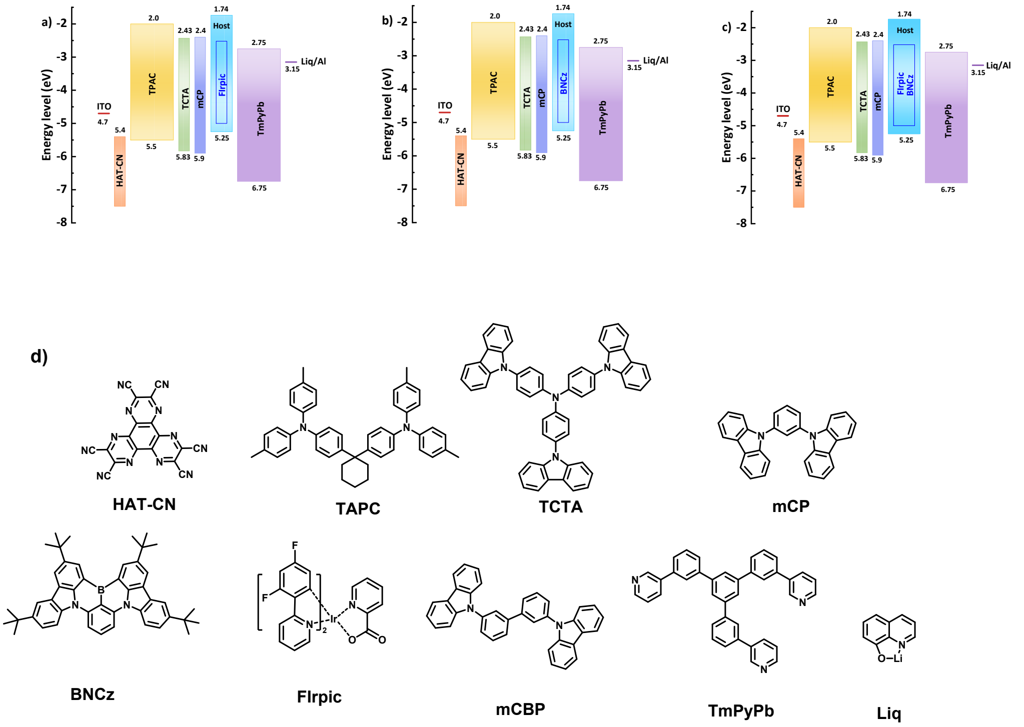

Figure S5. Energy level alignment of the device and the molecular structures of materials in different layers.

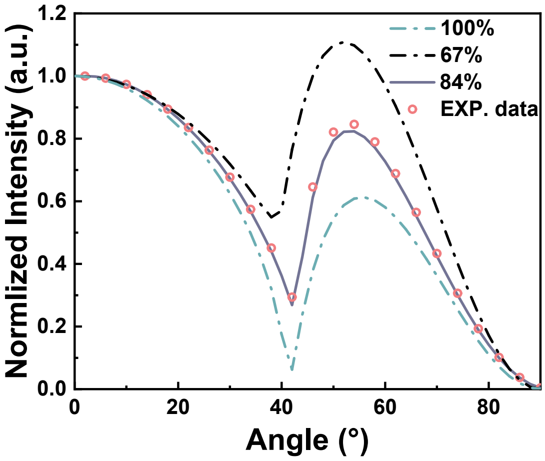

Figure S6. Angle-dependent *p*-polarized PL intensity and simulation curves of 15 wt% Firpic doped in **STFPPO**.

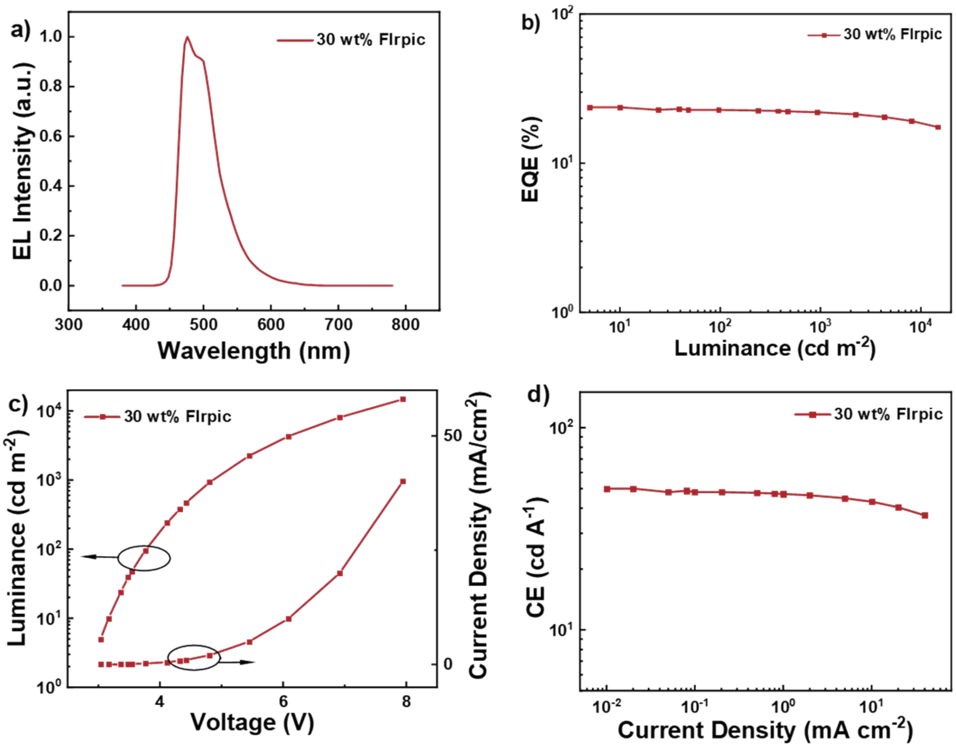

Figure S7. a) EL spectra at 5 mA cm^{-2}, b) External quantum efficiency versus luminance characteristics, c) Current density and luminance versus driving voltage characteristics, and d) Current efficiency versus current density characteristics of PHOLEDs using **STFPPO** as the host.

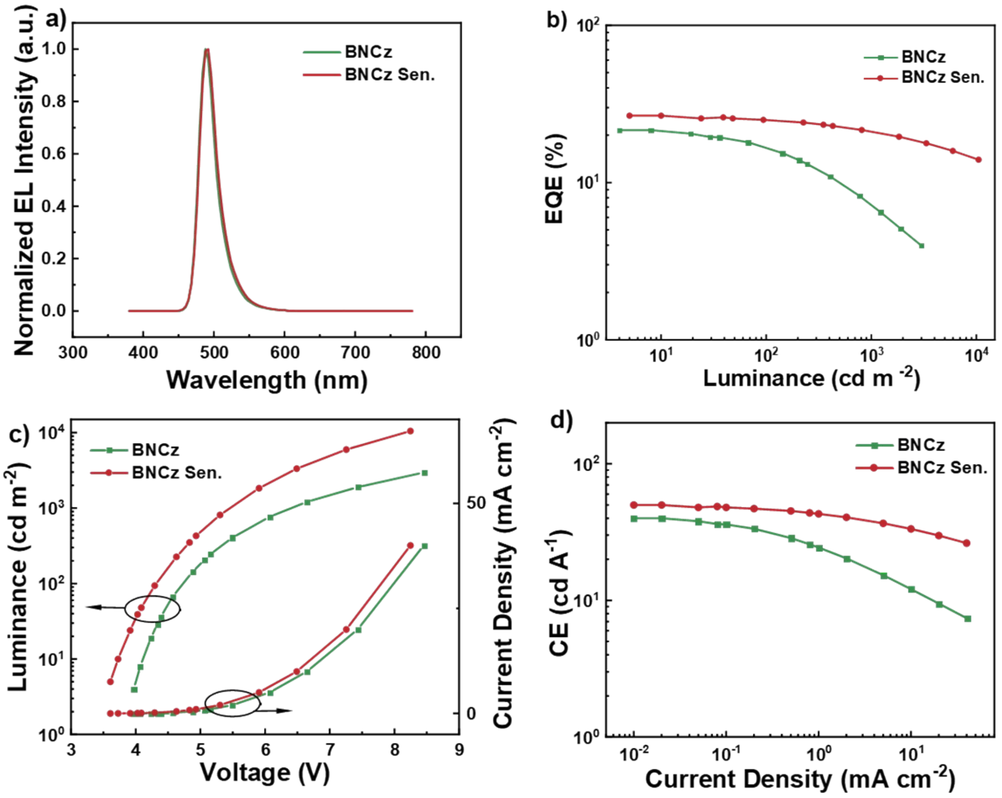

Figure S8. a) EL spectra at 5 mA cm^{-2}, b) External quantum efficiency versus luminance characteristics, c) Current density and luminance versus driving voltage characteristics, and d) Current efficiency versus current density characteristics of MR-TADF OLEDs using BNCz as the emitter and mCBP as host.

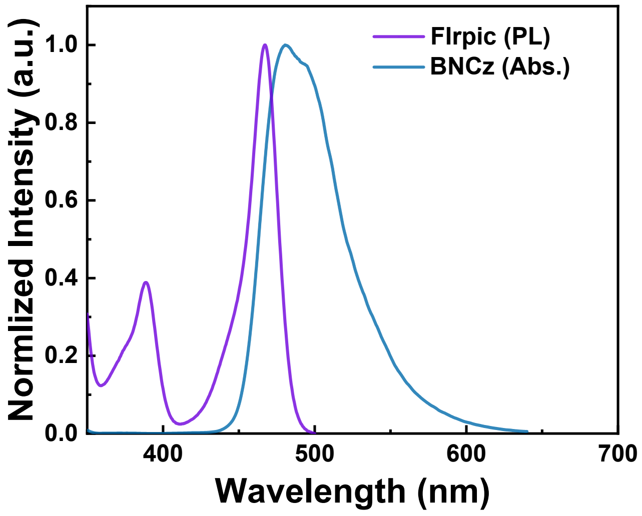

Figure S9. Spectral overlap region between FIrpic and BNCz in dilute toluene solution.

Table S3. Summary of BNCz-based device performances.

	λ_{EL} (nm)	CE (cd A^{-1})	PE (lm W^{-1})	EQE (%)	CIE (x, y)	Ref.
2 wt % BNCz: 15wt% FIrpic: STFPPO	**492**	**70**	**71.2**	**33.3**	**(0.09, 0.47)**	**This work**
0.5 wt % BNCz: 10 wt% f-t2empz: mCP	485	29.2	9.7	17.4	(0.12, 0.30)	[5]
1 wt% BNCz: mCBP	488	43.2	37.7	21.6	(0.10, 0.42)	[6]
1 wt% BNCz： 20 wt% CTPCF3： mCBP	488	-	-	27.5	(0.13, 0.40)	[7]
2 wt % BNCz: mCBP	490	-	-	27.8	(0.09, 0.40)	[8]
2 wt% BNCz: CzAcSF	490	31.1	19.5	16.3	-	[9]
3 wt% BNCz: 2,6-DCzPPy	488	-	27.4	20.5	-	[10]
3 wt% BNCz: 25 wt% 4TCzBN: mCBP	485	-	35.7	24.0	(0.10,0.30)	[11]

Synthesis and characterization

Synthesis of 1-(4-bromophenyl)-9H-fluoren-9-one

The compounds 9-fluorenone-1-boronic acid (4.00 g, 17.86 mmol), 1-bromo-4-iodobenzene (7.58 g, 26.78 mmol), tetrakis(triphenylphosphine)palladium(0) (1.03g, 0.89 mmol) and potassium carbonate (4.94 g, 35.71 mmol)were dissolved in THF/H_2O under Argon., and refluxed for 12 hours at 75 ^{o}C. The mixture was diluted with DCM and washed thrice with distilled water (200 mL). The organic layer was dried and purified through column chromatography using (petroleum ether/dichloromethane: 3/2, v/v as eluent) to obtain a yellow powder (4.36 g, 72%). ^{1}H NMR (400 MHz, Chloroform-*d*) δ 7.62 – 7.47 (m, 7H), 7.43 – 7.37 (m, 2H), 7.30 (td, *J* = 7.4, 1.1 Hz, 1H), 7.17 (dd, *J* = 7.4, 1.3 Hz, 1H). ^{13}C NMR (101 MHz, Chloroform-*d*) δ 192.95, 145.62, 143.47, 140.95, 136.30, 134.61, 134.36, 134.12, 131.28, 131.08, 130.82, 129.62, 129.33, 124.21, 122.60, 120.09, 119.55, 53.44. MS (EI) *m/z* calculated for $C_{19}H_{11}BrO$: 334.35, found:334.28 [M^+].

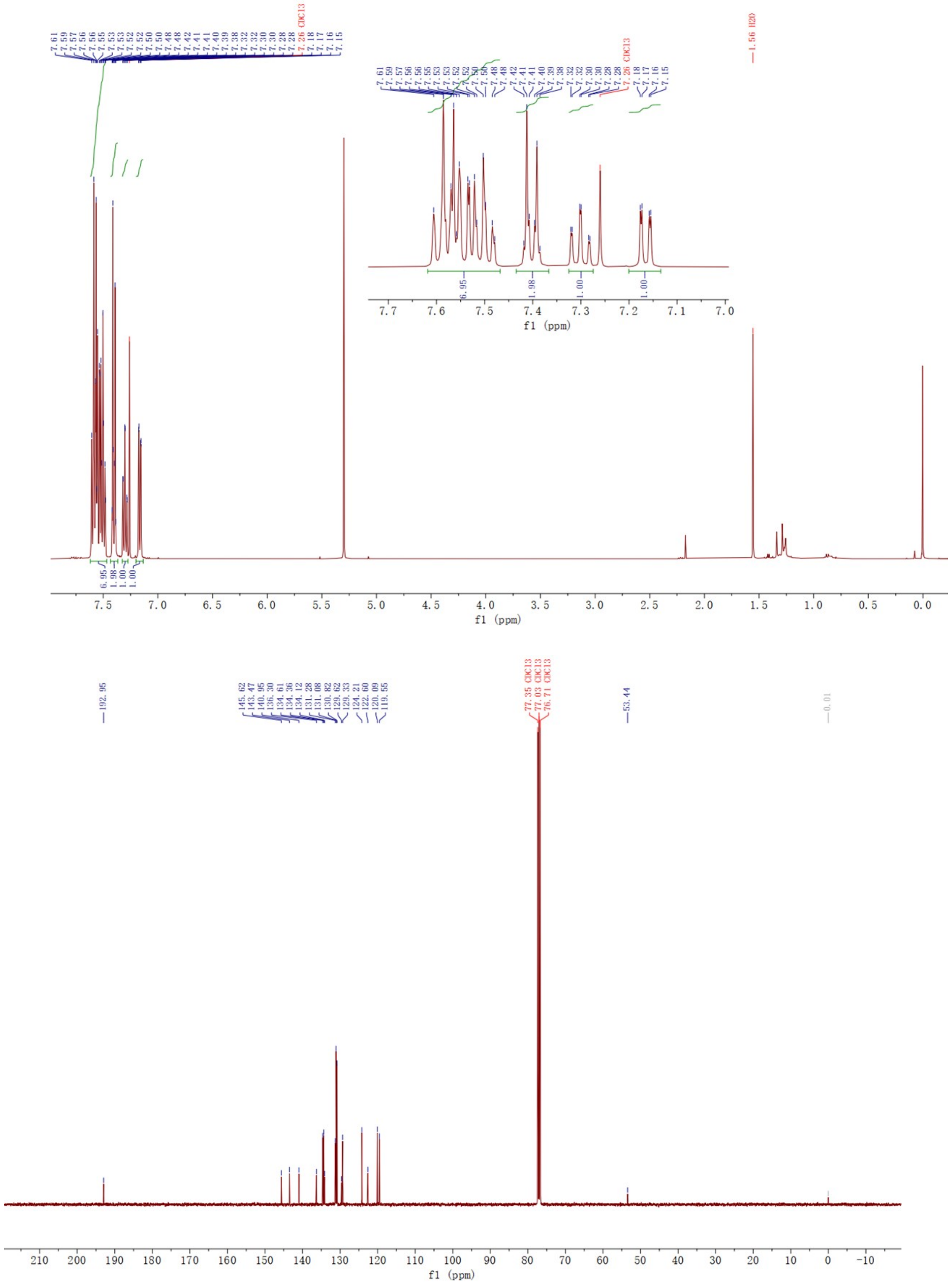

Figure S10. ^{1}HNMR and ^{13}CNMR spectra of 1-(4-bromophenyl)-9H-fluoren-9-one.

Synthesis of 1-PBr-STF

The compound 2-bromotriphenylamine (4.26 g, 13.13 mmol) was dissolved in anhydrous THF under Argon. The n-butyl lithium (1.6 M, 8.95 mL, 14.32 mmol) was added slowly at -78 ^{o}C, and the reaction mixture was stirred for 1 hour at the same condition. Then, anhydrous THF solution of 1-(4-bromophenyl)-9H-fluoren-9-one (4 g, 11.93 mmol) was added and further stirred for 2 hours at -78 ^{o}C. It was then stirred overnight at room temperature. After completion, the reaction mixture was quenched with anhydrous methanol (10 mL). And the organic solvent was removed by evaporation under reduced pressure. The resulting crude product was washed with water and submitted to flash column chromatography (PE/DCM: 5/2, v/v as eluent) to obtain a white powder (4.66 g, 67%), which was used in the next reaction after purification. The intermediate 2-(1-(4-bromophenyl)-9-methyl-9H-fluoren-9-yl)-*N*, *N*-diphenylaniline was dissolved in acetic acid (80 mL) refluxed at 110 ^{o}C for 20 minutes. Then, hydrochloric acid (8 mL) was added slowly to the reaction mixture. After 4 hours, a white solid appeared. It was filtered off and washed first with water and then petroleum ether (PE). Column chromatography was used for further purification (PE/DCM: 7/3, v/v as eluent) (4.38 g, 97%). ^{1}H NMR (400 MHz, Chloroform-d) δ 7.91 – 7.82 (m, 2H), 7.69 – 7.60 (m, 2H), 7.54 – 7.44 (m, 2H), 7.38 – 7.32 (m, 1H), 7.22 (d, J = 3.8 Hz, 2H), 7.12 – 7.06 (m, 4H), 6.99 (dd, J = 7.5, 1.1 Hz, 1H), 6.78 (td, J = 8.5, 7.1, 1.6 Hz, 2H), 6.51 – 6.43 (m, 2H), 6.30 (dd, J = 7.7, 1.6 Hz, 2H), 6.21 (d, J = 8.4 Hz, 2H), 5.94 (dd, J = 8.4, 1.2 Hz, 2H). ^{13}C NMR (101 MHz, Chloroform-d) δ 160.13, 155.56, 140.86, 140.51, 140.33, 139.80, 139.28, 137.78, 131.25, 131.08, 130.78, 129.96, 129.77, 128.80, 128.77, 128.14, 127.87, 127.19, 126.96, 126.23, 123.10, 120.74, 119.85, 119.24, 114.47, 56.11, 53.44. MS (EI) *m/z* calculated for $C_{19}H_{11}BrO$: 335.26, found: 335.18 [M^{+}].

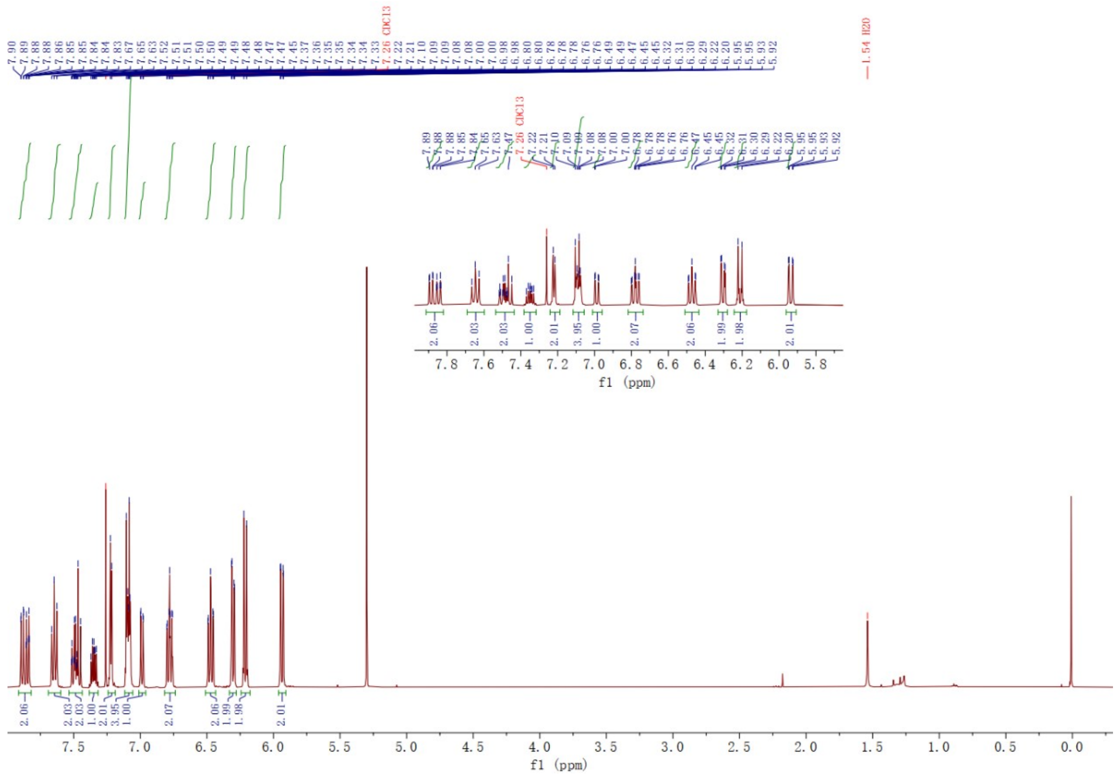

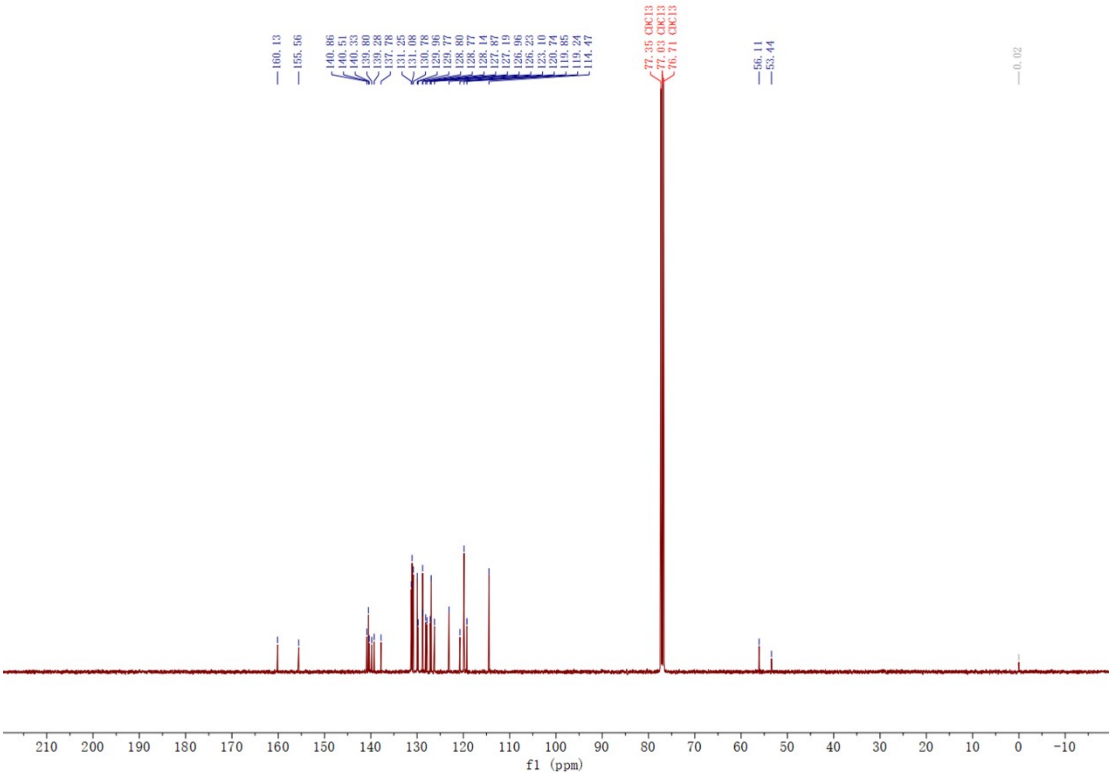

Figure S11. ^{1}HNMR and ^{13}CNMR spectra of 1-PBr-STF.

Synthesis of **STFPPO**

1-PBr-STF (2.0 g, 3.56 mmol) was dissolved in anhydrous THF under argon in Schlenk tube. The n-butyl lithium (2.5 mL/1.6 M, 3.91 mmol) was added drop wise to the solution under -78 °C. After one hour's stirring, diphenylphosphine chloride (1.18 g, 5.3 mmol) was added via a syringe. Then the resulting mixture was allowed to warm up to room temperature overnight. To terminate the reaction, 5 mL anhydrous methanol was added. And the organic solvent was removed by evaporation under reduced pressure. The resulting crude product was washed with water and submitted to flash column chromatography (PE/DCM: 6/1, v/v as eluent), affording the diphenylphosphine substituted intermediate as a white solid. Then the diphenylphosphine derivatives were dissolved in THF at room temperature. 3 mL H_2O_2 (30%) was added to the solution drop wise. After stirred at room temperature for 30 min, 50 mL water was added and organic layer was separated, dried, and evaporated under reduced pressure to afford the crude product. The crude products were further purified by recrystallization (using hexane and ethyl acetate as solvent) and vacuum sublimation. The final product is a white powder (1.72 g, 70.0%). ^{1}H NMR (400 MHz, Chloroform-*d*) δ 7.91 (dd, *J* = 7.6, 1.1 Hz, 1H), 7.82 (d, *J* = 7.6 Hz, 1H), 7.62 – 7.53 (m, 3H), 7.56 – 7.45 (m, 4H), 7.46 – 7.36 (m, 4H), 7.36 – 7.27 (m, 3H), 7.24 – 7.14 (m, 1H), 7.07 (d, *J* = 7.7 Hz, 2H), 6.79 – 6.69 (m, 3H), 6.59 (dd, *J* = 8.1, 2.7 Hz, 2H), 6.49 – 6.40 (m, 2H), 6.34 (dd, *J* = 7.8, 1.6 Hz, 2H), 5.96 (dd, *J* = 8.4, 1.2 Hz, 2H). ^{13}C NMR (101 MHz, Chloroform-d) δ 159.87, 154.65, 144.66, 144.63, 141.21, 140.59, 140.33, 139.82, 136.92, 133.37, 132.34, 132.16, 132.06, 131.85, 131.82, 131.23, 131.05, 130.87, 130.77, 130.27, 129.79, 129.23, 129.19, 129.06, 128.76, 128.48, 128.40, 128.36, 128.16, 128.11, 127.18, 126.90, 125.81, 123.49, 120.04, 119.96, 119.37, 114.62, 56.35. MS (MALDI-TOF) *m/z* calculated for $C_{49}H_{34}NOP$: 683.796, found: 683.241 [M^+].

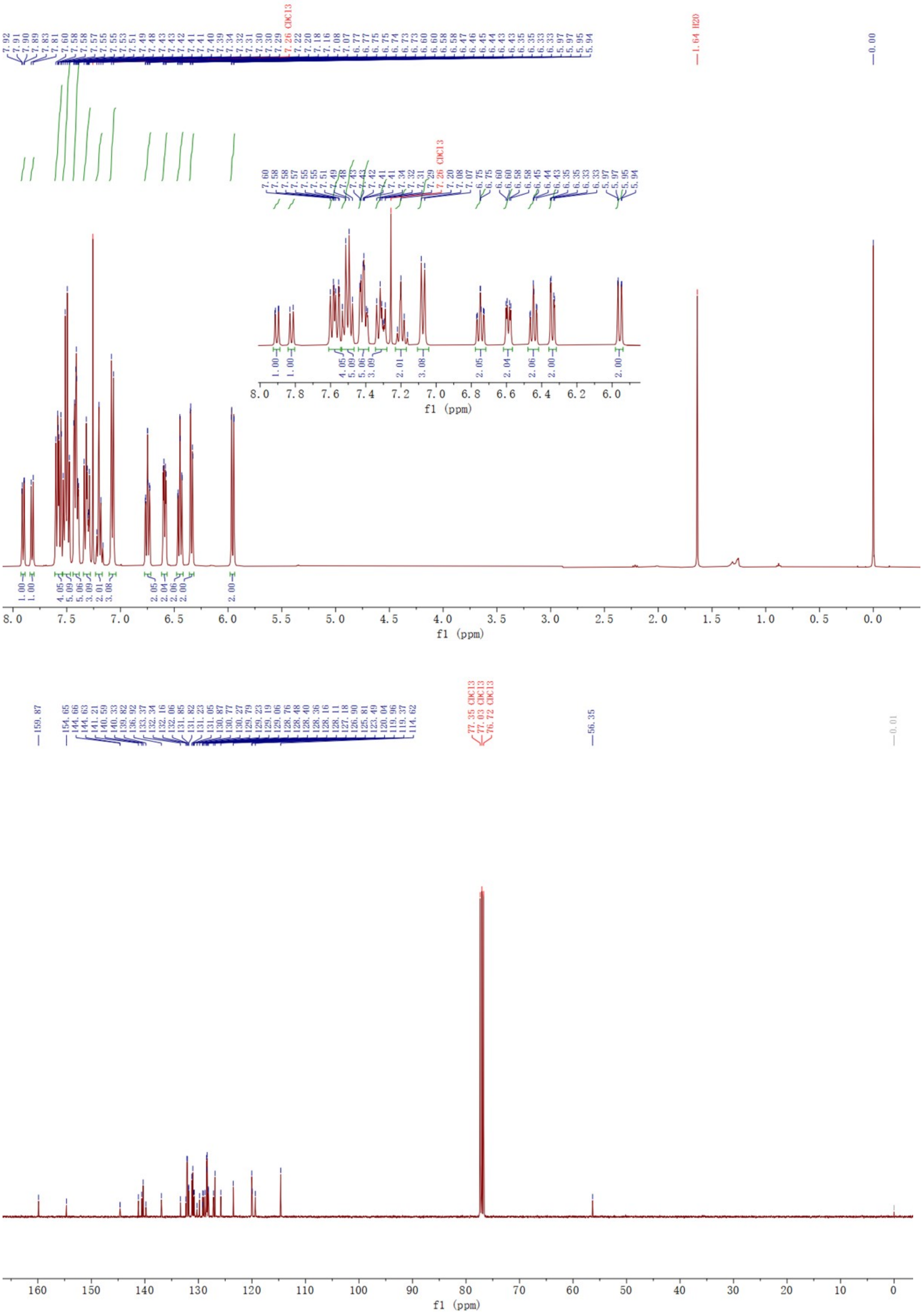

Figure S12. ^{1}HNMR and ^{13}CNMR spectra of **STFPPO**.

References

1. M. J. Frisch, G. W. Trucks, H. B. Schlegel, G. E. Scuseria, M. A. Robb, J. R. Cheeseman, G. Scalmani, V. Barone, G. A. Petersson, H. Nakatsuji, X. Li, M. Caricato, A. V. Marenich, J. Bloino, B. G. Janesko, R. Gomperts, B. Mennucci, H. P. Hratchian, J. V. Ortiz, A. F. Izmaylov, J. L. Sonnenberg, Williams, F. Ding, F. Lipparini, F. Egidi, J. Goings, B. Peng, A. Petrone, T. Henderson, D. Ranasinghe, V. G. Zakrzewski, J. Gao, N. Rega, G. Zheng, W. Liang, M. Hada, M. Ehara, K. Toyota, R. Fukuda, J. Hasegawa, M. Ishida, T. Nakajima, Y. Honda, O. Kitao, H. Nakai, T. Vreven, K. Throssell, J. A. Montgomery Jr., J. E. Peralta, F. Ogliaro, M. J. Bearpark, J. J. Heyd, E. N. Brothers, K. N. Kudin, V. N. Staroverov, T. A. Keith, R. Kobayashi, J. Normand, K. Raghavachari, A. P. Rendell, J. C. Burant, S. S. Iyengar, J. Tomasi, M. Cossi, J. M. Millam, M. Klene, C. Adamo, R. Cammi, J. W. Ochterski, R. L. Martin, K. Morokuma, O. Farkas, J. B. Foresman and D. J. Fox, 2016. Gaussian, Inc., Wallingford CT.
2. F. Neese, *WIREs Comput. Mol. Sci.*, 2018, **8**, e1327.
3. F. Weigend and R. Ahlrichs, *Phys. Chem. Chem. Phys.*, 2005, **7**, 3297-3305.
4. J.-D. Chai and M. Head-Gordon, *Phys. Chem. Chem. Phys.*, 2008, **10**, 6615-6620.
5. J. Yan, Q. Xue, H. Yang, S.-M. Yiu, Y.-X. Zhang, G. Xie and Y. Chi, *Inorg. Chem.*, 2022, **61**, 8797-8805.
6. Y. Xu, Z. Cheng, Z. Li, B. Liang, J. Wang, J. Wei, Z. Zhang and Y. Wang, *Adv. Opt. Mater.*, 2020, **8**, 1902142.
7. Y. Zhang, J. Wei, D. Zhang, C. Yin, G. Li, Z. Liu, X. Jia, J. Qiao and L. Duan, *Angew. Chem. Int. Ed.*, 2022, **61**, e202113206.
8. M. Yang, I. S. Park and T. Yasuda, *J. Am. Chem. Soc.*, 2020, **142**, 19468-19472.
9. S. Xu, Q. Yang, Y. Zhang, H. Li, Q. Xue, G. Xie, M. Gu, J. Jin, L. Huang and R. Chen, *Chin. Chem. Lett.*, 2021, **32**, 1372-1376.
10. B. Lei, Z. Huang, S. Li, J. Liu, Z. Bin and J. You, *Angew. Chem. Int. Ed.*, 2023, **62**, e202218405.
11. X. Xiao, B. Lei, D. Wu and Z. Bin, *Chem. Commun.*, 2023, **59**, 6556-6559.